1 **Development, characterization and application of an improved online**

2 **reactive oxygen species analyzer based on MARGA**

3 Jiyan Wu[1,2], Chi Yang[1,2], Chunyan Zhang [1,2], Fang Cao[1,2], Aiping Wu[1,2], Yanlin Zhang[1,2]

4 *

5 [1] *Yale-NUIST Center on Atmospheric Environ., Joint International Research*
6 *Laboratory of Climate and Environment Change (ILCEC), Nanjing University of*
7 *Information Science and Technology, Nanjing 210044, China*
8 [2] *School of Applied Meteorology, Nanjing University of Information Science and*
9 *Technology, Nanjing 210044, China*
10 *Correspondence: Yanlin Zhang (zhangyanlin@nuist.edu.cn)*

11

12 **Abstract**

13   Excessive reactive oxygen species (ROS) in the human body is an important factor
14 leading to diseases. Therefore, research on the content of reactive oxygen species in
15 atmospheric particles is necessary. In recent years, the online detection technology of
16 ROS has been developed. However, there are few technical studies on online detection
17 of ROS based on the DTT method. Here, to modify the instrument, it is added a DTT
18 experimental module that is protected from light and filled with nitrogen at the end,
19 based on the Monitor for AeRosols and Gases in ambient Air (MARGA). The
20 experimental study found that the detection limit of the modified instrument is 0.024
21 nmol min^{-1}. And the accuracy of the online instrument is determined by comparing the
22 online and offline levels of the samples, which yielded good consistency (slope 0.97,
23 R^2=0.95). It shows that the performance of the instrument is indeed optimized, the
24 instrument is stable, and the characterization of ROS is accurate. The instrument not
25 only realizes the online detection conveniently and quickly, but also achieves the hour-
26 by-hour detection of ROS based on the DTT method. Meanwhile, reactive oxygen and
27 inorganic ions in atmospheric particles are quantified using the online technique in the
28 northern suburbs of Nanjing. It is found that the content of ROS during the day is higher
29 than that at night, especially after it rains, ROS peaks appear in the two time periods of
30 08:00-10:00 and 16:00-18:00. In addition, examination of the online ROS and water-
31 soluble ions (SO_4^{2-}, NO_3^-, NH_4^+, Na^+, Ca^{2+}, K^+), BC and polluting gases (SO_2, CO, O_3,
32 NO, NO_x) measurements revealed that photo-oxidation and secondary formation
33 processes could be important sources of aerosol ROS. This method breakthrough
34 enables the quantitative assessment of atmospheric particulate matter ROS at the
35 diurnal scale, providing an effective tool to study sources and environmental impacts
36 of ROS.

37 **1、Introduction**

38   Air quality is a major issue affecting human health, and prolonged exposure to
39 high ambient particulate concentrations can lead to a significant increase in the
40 probability of respiratory and cardiovascular diseases, which can seriously impair
41 human health (Delfino et al., 2005; Ghio et al., 2012; Pöschl and Shiraiwa, 2015). The
42 production of reactive oxygen species (ROS) in the human body is the most reliable

Atmospheric
Measurement
Techniques
Discussions
Open Access
EGU

43 pathophysiological mechanism proposed, and excessive reactive oxygen species can
44 cause an imbalance between the oxidative system and the antioxidant system, causing
45 oxidative stress and tissue damage (Ahmad et al., 2021; Akhtar et al., 2010; Borm et al.,
46 2007; Delfino et al., 2013; Lodovici and Bigagli, 2011). Thus, oxidative potential (OP)
47 has been proposed as a more biologically relevant indicator than particulate matter (PM)
48 mass concentration to represent the combined effects of multiple toxic components in
49 PM (Ayres et al., 2008; Hellack et al., 2015; Janssen et al., 2015). Understanding the
50 generation mechanism and source characteristics of reactive oxygen species is essential
51 for making reasonable pollution control decisions and reducing their impact on human
52 health.
53   In recent years, the analysis method of oxidation potential has cell detection and
54 cell-free detection. To provide a simpler and quicker way to determine the oxidation
55 potential of environmental particulate matter, cell-free methods such as electron spin
56 (or paramagnetic) resonance (OP_{ESR}), dithiothreitol assay (OP_{DTT}), ascorbic acid assay
57 (OP_{AA}), high-performance liquid chromatography (HPLC) and glutathione assay
58 (OP_{GSH}) are often used as the main measurement methods for ROS (Bates et al., 2019;
59 Ghio et al., 2012). Through the comparison and analysis of these various methods by a
60 large number of researchers, the DTT method is generally considered to be the most
61 common and comprehensive method to reflect the magnitude of the chemical oxidation
62 potential of particulate matter (Hedayat et al., 2014; Xiong et al., 2017).
63   Generally, the cell-free method still has problems with detection delays and
64 degradation of particulate chemical components during sample storage, which not only
65 leads to inaccurate detection data, but also the inability to capture daily changes.
66 Therefore, the development of online detection technology becomes necessary
67 (Charrier et al., 2016; Dou et al., 2015; Fang et al., 2017; Li et al., 2012; Liu et al., 2014;
68 Velali et al., 2016; Vreeland et al., 2017). So far, the development of online detection
69 technology is mainly based on the DCFH method and the DTT method. On the one
70 hand, an online detection technology based on the DCFH method has been reported
71 previously (Eiguren-Fernandez et al., 2017; Huang et al., 2016; Sameenoi et al., 2012;
72 Wragg et al., 2016). However, some researchers believe that in the DCFH method, the
73 horseradish peroxidase (HRP) will promote the production of hydroxyl free radicals,
74 leading to an overestimation of ROS content (Pal et al., 2012). On the other hand, based
75 on the DTT method to develop online detection technology (Fang et al., 2014;
76 Puthussery et al., 2018), The semi-automatic detection system researched by Fang et al,
77 based on the DTT method cannot realize an online collection of environmental samples.
78 On this basis, Puthussery et al used a mist chamber (MC) to continuously collect $PM_{2.5}$
79 in environmental water and realized fully automatic hourly ROS detection.
80   However, these detection methods ignore the influence of air and light on the
81 experiment. As the main reagent of the experiment, dithiothreitol (DTT) and 5,5'-
82 dithiobis (2-nitrobenzoic acid) (DTNB) are easily oxidized by air (Chen et al., 2010).
83 Therefore, this experiment is optimized based on the research of Fang et al and
84 Puthussery et al. We achieve accurate measurement of the oxidation potential of
85 environmental particulates by shielding from light and filling with nitrogen. In addition,
86 the present study is developed on the basis of the MARGA, which is a reliable field

87 instrument. And it is not only used in many research institutes for long-term ion
88 observation but also used to transform the observation of low-molecular-weight organic
89 acids in the gas and particle phases (Stieger et al., 2019). MARGA is used to collect
90 particulate matter and is connected to the optimized DTT_V detection part to observe the
91 oxidation potential hour by hour. The system realizes simultaneous observation of
92 oxidation potential and inorganic ions. Here, we optimize the performance of the
93 instrument and measure the hourly averaged OP of ambient $PM_{2.5}$. The reliability of
94 online detection of oxidation potential data is supported by analyzing the correlation
95 between ions, polluting gases, BC and oxidation potential.

96 ## 2、 Materials and Method

97 ### 2.1 Instrument set-up and improvement

98 Figure 1 shows the scheme and schematic diagram of the system for DTT online
99 detection. The instrument is set up in the Atmospheric Environ. monitoring laboratory
100 on the roof of the Wende Building of Nanjing University of Information Engineering
101 (30 m above the ground) and the room temperature is maintained at 20°C. The entire
102 system is composed of the MARGA, the automatic sample-receiving device, and the
103 DTT experimental reaction device. The MARGA is used as an instrument for detecting
104 atmospheric aerosols and inorganic components of gases (water-soluble ions Cl^-、NO_3^-、
105 SO_4^{2-}、NH_4^+、Na^+、K^+、Mg^{2+}、Ca^{2+}), and it collects gases using a wet rotary separator
106 and aerosols using steam injection, and absorbs gases and aerosols into the aqueous
107 phase separately to separate them from each other. Then, the resulting solution is
108 analyzed by ion chromatography equipped with a conductivity detector. That is, the gas
109 and aerosol are analyzed separately to detect the gas precursors and different ionic
110 compositions in the aerosol.

111 In the DTT reaction module, to avoid the influence of light and air on the
112 experiment, the DTT experimental part in this experiment was kept in an environment
113 protected from light and flushed into nitrogen. In addition, we added a refrigerator to
114 store DTT, DTNB and other experimental solutions. During the DTT experiment, the
115 reaction tube and mixing tube were placed in an incubator at 37°C to simulate the
116 temperature of human lungs. To realize the subsequent DTT experimental reactions, as
117 in Figure 1 we collected the liquid-phase aerosols into sample tubes through a dual-
118 channel split-flow controlled-volume peristaltic pump. And set peristaltic pump 1 speed
119 to 1.55 ml h^{-1} to finish 1.5 ml h^{-1} sample volume.

120 Finally, the determination of DTT activity is achieved by the continuous regular
121 operation of the programmable pumps A and B and the detection of the
122 spectrophotometer. (see Sect. 2.2.1 for details)

123 ### 2.2 Method

124 ### 2.2.1 Online DTT assay measurement

125 The whole measurement step is divided into three steps: sample collection, DTT
126 reaction part, and spectrophotometer detection. In the first step (the sample collection),
127 the MARGA will discharge 25 ml of aerosol liquid every hour, and use the dual-channel
128 split flow control volume peristaltic pump 1 to add 1.55 ml of the solution (to ensure

129   1.5 ml of sample) into the sample tube, and the rest will enter the automatic sampling
130   device to save through the peristaltic pump 2 (the automatic sampler is set to rotate one
131   grid per hour).
132   In the second step (the part is protected from light and in a nitrogen environment),
133   the reaction part is divided into a DTT oxidation step and a DTT determination
134   step(Wang et al., 2019). First (DTT oxidation step), use pump A to add 5 mL potassium
135   phosphate buffer (0.1 mol L^{-1}), 1.5 mL aerosol extract sample, and 0.5 mL DTT (1
136   mmol L^{-1}) into the mixing bottle (MV) in sequence. Inhale ultrapure water to clean the
137   syringe of pump A. DTT reacts with the aerosol extract in MV. Second (DTT
138   determination step), after completing the first step, immediately use pump A to pump
139   1mL TCA (10% w/v; quencher) into the reaction flask (RV, wrap it in aluminum foil to
140   prevent possible Light interference). Then, use pump A to suck the mixed solution in
141   the 1ml mixing bottle and transfer it to the reaction bottle to mix it with TCA. Add 0.05
142   mL DTNB (0.01 mmol L^{-1}) via pump B and mix. The residual DTT reacts with DTNB
143   to form light absorption product 2-nitro-5-thiobenzoic acid (TNB) with high extinction
144   performance at 412 nm.
145   In the third step, in the detection part of the spectrophotometer, use pump A to add
146   4 mL Tris buffer (0.4 mol L^{-1}, containing 20 mmol L^{-1} EDTA) into the reaction flask
147   (RV). After the reaction is completed, use pump A to add the final mixture solution in
148   the reaction flask to the LWCC for the absorbance test. The data acquisition software
149   (Spectra Suite) records the absorbance at 412 and 700 nm every 10 min (select the
150   baseline absorbance of TNB). Then, the system uses deionized water (deionized water)
151   for self-cleaning to eliminate any residual liquid in the reaction flask, tubing, syringe,
152   and LWCC. To determine the rate of DTT consumption, the time interval is 10 min, and
153   a total of 6 (0 min, 10 min, 20 min, 30 min, 40 min, 50 min) data points of DTT
154   concentration over time are generated. Finally, the automated system performs the self-
155   cleaning procedure again to ensure that there is no residue, and the system repeats the
156   above operations in the next hour to realize hourly detection of DTT activity.

$$\Delta DTT = -\sigma Abs \cdot \frac{N_0}{Abs_0} \qquad (1)$$

$$DTTv = \frac{\Delta DTT_s(nmol\ min^{-1}) - \Delta DTT_b(nmol\ min^{-1})}{V_t(m^3) \times \frac{V_s(mL)}{V_e(mL)}} \qquad (2)$$

159   where σAbs is the slope of absorbance versus time; Abs$_0$ is the initial absorbance
160   calculated from the intercept of the linear regression of absorbance versus time; and N$_0$
161   is the initial moles of DTT added in the reaction vial. ΔDTT_s(nmol min^{-1}) is the DTT_v
162   consumption rate of the sample, ΔDTT_b(nmol min^{-1}) is the blank DTT consumption
163   rate, $V_t(m^3)$ is the sampling volume corresponding to the sample, and V_s(mL) is the
164   injection volume, V_e(mL) is the sampling volume.

165   **2.2.2 Online DTT instrument performance**
166   The performance of the automated system is characterized by testing to determine
167   the instrument response, limit of detection (LOD), precision and accuracy, while using
168   a large flow sampler to collect samples for offline and online comparative analysis. (See
169   Sect.3.1 for details)
170   We perform DTT activity detection and comparison on samples collected by 9,10-

171   phenanthraquinone（PQN）and traditional high-flow samplers. First, we select PQN

172   with concentrations of 0.01, 0.02, 0.025, 0.05, 0.085 nmol L^{-1} to compare online and

173   offline DTT activity detection to determine the error of online and offline experiments.

174   Secondly, select 10 traditionally collected samples for online and offline comparison,

175   and then combine the experimental error between online and offline determined by

176   PQN (PQN online and offline orthogonal fitting) to analyze the accuracy of online and

177   offline.

178   **2.2.3 Instrument maintenance**

179   DTT and DTNB solutions are prepared once every 4 days, and the rest of the

180   solutions are prepared according to the amount. Before each test, perform an overall

181   light-proof and nitrogen bag inspection. The standard curve was measured once before

182   each experiment. PQN is calibrated online and offline ever month. Clean the instrument

183   pipeline once a week, 5 times each time (Ultra-pure water).

184   **2.3 Collection and preparation of environmental samples**

185   The sampling point is located on the roof of the seventh floor of the Maintenance

186   Branch (34°58′ N, 117°26′ E) of the Power Company, Yunlong District, Xuzhou City.

187   The surrounding buildings mainly include auto repair shops, logistics centers,

188   pharmaceutical factories, and large residential areas and farmland. A large flow $PM_{2.5}$

189   sampler (KC-6120) is used for continuous sampling, and a total of 10 samples are

190   collected (October 21, 2018-October 31, 2018). When sampling, the flow rate is 1.0 m^3

191   min^{-1}, and each sampling time is 24 h; in this study, we collected samples using quartz

192   filters and stored them in a refrigerator at -26 °C. Before the start of the experiment, the

193   collected samples were subjected to extraction processing, and a sample film with a

194   diameter of 16 mm is cut into a brown glass bottle, 5 ml ultrapure water is added to

195   shake for 30 min, and filtered with a 0.22 μm PTFE syringe filter to remove insoluble

196   substances.

197   **3. Results and discussion**

198   **3.1 Instrument performance**

199   **3.1.1 Improvement of the instrument**

200   As we all know, photo-oxidation promotes the generation of ROS (Fang et al.,

201   2016; Visentin et al., 2016; Yang et al., 2014). In addition, during the measurement

202   process, the ingress of air inside the instrument will also cause the DTT activity to

203   increase. Therefore, before on-site deployment, the online DTT inspection instrument

204   was optimized by filling in nitrogen gas and shielding the whole from light. And

205   respectively detect the DTT consumption rate (ΔDTT) of 10 blanks (ultra-pure water)

206   before and after optimization. As shown in Figure 2, before the system optimization,

207   we found that the average ΔDTT measured by 10 blanks was 0.25±0.04 nmol min^{-1},

208   and there is a big fluctuation. After optimization, the average ΔDTT is 0.14±0.008 nmol

209   min^{-1}, which is significantly lower than system optimization. Moreover, the standard

210   deviation (0.008) is much smaller than Puthussery et al (0.08) and Fang et al (0.103)

211   (Fang et al., 2014; Puthussery et al., 2018). It shows that air and light do promote the

212   generation of ROS, and the nitrogen environment and avoiding light contribute to the

Atmospheric
Measurement
Techniques
Discussions

Open Access

EGU

213   stability of the system. The optimized system is more accurate in measuring the
214   oxidation potential of environmental particulate matter. To further prove the
215   optimization effect, the performance of the instrument is studied. (See Sect.3.1.4 for
216   details)

217   **3.1.2 Calibration of DTTv measurement and analysis system**

218   In past studies, PQN is often used as a standard sample of atmospheric particulate
219   matter (Charrier and Anastasio, 2011; Charrier and Anastasio, 2015; Xiong et al., 2017).
220   The analytical measurement part of the online DTT instrument is calibrated by
221   measuring the DTT activity of PQN at different concentrations. As shown in Figure 3,
222   the linear graph of DTT consumption rate and PQN concentration, the online detection
223   slope is 3.66±0.26, and the coefficient R^2=0.992. The calibration slope is less than the
224   slope obtained by the automatic DTT system of Fang et al. (2015) and Puthussery et al
225   (2018). This also shows that shielding from light and filling with nitrogen will reduce
226   DTT consumption, and it also supports the accuracy of the system in determining the
227   oxidation potential of environmental particulates. During the on-site operation, PQN's
228   online and offline testing is measured at least once a month to ensure online accuracy.

229   **3.1.3 Limit of detection and precision**

230   The limit of detection (LOD) of the system is defined as 3 times the standard
231   deviation of the deionized water blank (N = 23), which is 0.024 nmol min^{-1}. To ensure
232   the accuracy of the system, the deionized water blank samples are taken once a day (14
233   days) during the sampling period, besides the 10 continuously measured during the
234   optimization of the system.

235   Use deionized water to evaluate the accuracy of the environmental sample
236   automation system and analyze the DTT activity. The low standard deviation
237   (coefficient of variation, CV=5.61%) of 0.024 nmol min^{-1} indicates that the system has
238   sufficiently high accuracy for environmental samples.

239   **3.1.4 Accuracy**

240   The accuracy of the system is verified by comparing the DTT activity of the
241   positive control and environmental particulate samples obtained from the automated
242   method with the results obtained from the same experimental protocol performed
243   manually. (Cho et al., 2005)

244   Five concentrations of PQN solutions (0.01, 0.02, 0.025, 0.05, 0.085 nmol L^{-1}) are
245   run in the automatic system, which is very close to the results of the manual system (the
246   standard deviation of the automatic system is kept at 0.008 nmol min^{-1}, and the
247   coefficient of variation is 2.28 %; the standard of the manual system The difference is
248   0.0044 nmol min^{-1}, the coefficient of variation is 1.48 %). As shown in Figure 4, the
249   slope (manual/automatic) obtained by orthogonal fitting is 1.14, the intercept is 0.12,
250   and the correlation coefficient (R^2) is 0.997. To ensure the high accuracy of the online
251   system and the offline system, as a further verification, we used online and offline
252   manual methods to conduct DTT activity analysis on ten environmental particulate
253   matter samples.

254   We use the PQN online and offline DTT consumption rate orthogonal fitting result
255   as the system to correct the error, as shown in Figure 5, through the offline and online
256   orthogonal fitting of 10 environmental particulate matter samples before and after the

257 error correction. We found that the corrected results are better (the slope is 0.97 closer
258 to 1, the intercept is 0.05 closer to 0, R^2=0.954), which is significantly better than the
259 results of Puthussery et al. The good agreement between the two sampling systems
260 indicates that the DTT measurement of environmental samples has high overall
261 accuracy. These tests also proved the necessity of optimization.

262 **3.2 DTT activity of ambient samples**

263 　　The volume-normalized oxidation potential DTT_V is used as an index of exposure
264 to inhaled air to point out the inherent ability of particles to deplete relevant antioxidants.
265 During the observation period, the daily change of DTT_V in Nanjing is shown in Figure
266 6. The average DTT_V is 0.83±0.38 nmol min^{-1} m^{-3}. Compared with Beijing's DTT_V in
267 the spring of 2012 (urban area: 0.24 nmol min^{-1} m^{-3})(Liu et al., 2014; Wang et al., 2019).
268 and Zhejiang University's annual DTT_V average of 0.62 nmol min^{-1} m^{-3}(Yu et al., 2019) ,
269 our results are on the high side; And compared with Peking University's 2015 annual
270 DTT_V (12.26±6.82 nmol min^{-1} m^{-3}) (Perrone et al., 2016)and Guangzhou's In the winter
271 of 2017 (DTT_V: 4.67±1.06 nmol min^{-1} m^{-3}) and in the spring of 2018 (DTT_V: 4.45±1.02
272 nmol min^{-1} m^{-3}), our values are low, which may be related to the current season and
273 emission factors. In addition, we found that the rain during the sampling period caused
274 significant changes in the 24-hour DTT_V. To better understand the environmental
275 factors affecting DTT_V, we divided the DTT_V daily activities. As shown in Figure S2,
276 the daily distribution of 24-hour DTT activities during the entire sampling period (a),
277 before rain (b), during rain (c), and after rain (d) are divided. Figure S2(a) represents
278 the hourly change of DTT_V during the entire sample period. We found that the highest
279 value of DTT_V in a day occurs at 11-12 am, and DTT_V is greater during the day than at
280 night, which is similar to the study by Puthussery et al. Before the rain, the average
281 DTT_V was 0.81±0.17 nmol min^{-1} m^{-3}. There is a peak at 10-12 am, but the overall
282 situation is relatively flat, and there is no obvious difference between day and night.
283 And the average value of DTT_V during the rain is 0.55±0.10 nmol min^{-1} m^{-3}, which
284 decreased significantly. There is no doubt that this is caused by rain settling the
285 polluting components of the atmosphere. In contrast, there is significant daily activity
286 in DTT_V following rain, with peaks occurring mainly between 8-10 am and 4-6 pm, and
287 DTT_V is significantly higher during the day than at night, which is similar to the
288 Puthussery study (Puthussery et al., 2018).

289 **3.3 The correlation between $PM_{2.5}$ and polluting gases and ROS activity**

290 　　To further study, the daily changes of DTT_V and its correlation with various
291 emission sources on site. As shown in Figure 7, we measured the water-soluble ionic
292 components of $PM_{2.5}$ (SO_4^{2-}, NO_3^-, NH_4^+, Na^+, Ca^{2+}, K^+), BC, and pollution gas (SO_2,
293 CO, O_3, NH_3) content changes. The average concentration of $PM_{2.5}$ during the sampling
294 period was 9.97±6.53 ng m^{-3}, the average concentration of $PM_{2.5}$ before rain was
295 11.13±7.21 ng m^{-3}, the average concentration of $PM_{2.5}$ after rain was 7.80±4.18 ng m^{-3},
296 $PM_{2.5}$ There is a significant drop in concentration. And through correlation analysis, we
297 found that DTT_V and $PM_{2.5}$ concentration were positively correlated before rain, but
298 negatively correlated after rain. Therefore, we suspect that the source of DTT_V is
299 different before and after the rain. BC and the polluting gases SO_2, NO_x, NO_2, CO, Ca^{2+},
300 K^+, Mg^{2+} are often used as tracers of biomass burning, coal combustion, and dust storms.

301 The levels of these substances were not high during the sampling period and decreased
302 to varying degrees after rain. It is similar to Liu and Zhang et al who concluded that
303 biomass burning, coal combustion, and dust storms were not major sources of pollution
304 in Nanjing during the summer(Guo et al., 2019; Liu et al., 2019; Zhang et al., 2020). In
305 addition, there was no strong correlation between DTT_V and SO_2, NO_x, NO_2, and CO
306 before and after the rain. Therefore, it can be judged that neither biomass burning, coal
307 combustion nor dust is the main source affecting DTT_V. In contrast, we found that there
308 is a significant difference between day and night in O_3 after rain, which is similar to the
309 change of DTT_V, and after rain, DTT_V and O_3 show a strong correlation (r=0.624). After
310 it rains, the O_3 content in the air environment increases. Under the action of the sun's
311 ultraviolet rays, the O_3 is photodegraded to form active oxygen components such as OH
312 radicals (Ehhalt and Rohrer, 2000; Rohrer and Berresheim, 2006).
313 To further confirm the influence of light on DTT_V, the day and night correlation
314 analysis of substances related to photo-oxidation (NH_4^+, NO_3^-, SO_4^{2-}) and DTT_V is
315 carried out. As shown in Table S2, we find that NH_4^+, NO_3^-, SO_4^{2-} and DTT_V are
316 significantly correlated during the day (r=0.434, r=0.461, r=0.263, P<0.01). As far as
317 we know, there is no evidence in the literature that water-soluble inorganic ions (NH_4^+,
318 NO_3^-, SO_4^{2-}) have redox activity in an aerobic environment(Calas et al., 2018;
319 Stevanovic et al., 2017). However, their correlation with DTT_V may be due to
320 collinearity with redox-active organic compounds, rather than actual contribution to the
321 oxidation potential of particles. We speculate that the high correlation may be related
322 to the photochemical reactions that occur during the day.

4、Summary and conclusions

324 This study proposes and characterizes an improved online active oxygen analyzer.
325 Compared with the previous research, the main improvements(Fang et al., 2014;
326 Puthussery et al., 2018). The optimization analysis is as follows: (1) The experimental
327 environment is processed to isolate the air and avoid light; (2) The sampling method
328 has changed. We use the MARGA online ion analyzer, which is more mature and stable.
329 Compared with before optimization, the standard deviation of the blank was
330 significantly smaller, Thus, the detection limit of the instrument (0.024 nmol min^{-1})
331 becomes smaller and more stable. The DTT consumption rate is reduced by 24.4 %,
332 which eliminates the influence of outside air and light in the experiment. And the
333 consistency between online and offline is improved (slope=0.97, R^2=0.95), the
334 accuracy of the system is higher.
335 By changing the DTT_V content hour by hour during the sampling period, we found that
336 the DTT activity during the day is higher than that at night, and it is especially obvious
337 after rain, which is mainly related to the increase in UV radiation during the day after
338 rain. In addition, we analyzed the correlation between water-soluble ions (SO_4^{2-}, NO_3^-,
339 NH_4^+, Na^+, Ca^{2+}, K^+), BC, pollutant gases（SO_2, CO, O_3, NO, NO_x, NH_3） and DTT_V,
340 and we found that the main source of influence of OP in the Nanjing environment in
341 summer is daytime Secondary photochemical conversion and ultraviolet radiation. In
342 the future, we hope to add more experimental modules to the back-end based on the
343 MARGA sample collection device to realize the diversification of detection
344 compositions. In addition, the system can be combined with other substance detection

345   instruments. It will achieve the daily contribution of various emission sources to the

346   risk associated with OP exposure can be inferred from other species.

347

348 *Data availability.* Data used in this paper can be provided upon request by email to
349 ZYL (dryanlinzhang@outlook.com) .

350 *Author contributions*. WJY designed the instrument, led the sampling campaign,
351 performed the experiments, and wrote the manuscript. YC participated in experimental
352 design and guided the experimental process. ZCY chose the building address and
353 initially built the instrument. CF helped in the filter collection and in conducting the
354 DTT activity experiments. ZYL conceived the idea, organized the manuscript, and
355 supervised the project.

356 *Competing interests*. The authors declare that they have no conflict of interest.

361

Atmospheric
Measurement
Techniques

Open Access

EGU

Discussions

References:

Ahmad, M., Yu, Q., Chen, J., Cheng, S., Qin, W., and Zhang, Y.: Chemical characteristics, oxidative potential, and sources of PM (2.5) in wintertime in Lahore and Peshawar, Pakistan, J Environ Sci (China), 102, 148-158, https://doi.org/10.1016/j.jes.2020.09.014, 2021.

Akhtar, U. S., McWhinney, R. D., Rastogi, N., Abbatt, J. P., Evans, G. J., and Scott, J. A.: Cytotoxic and proinflammatory effects of ambient and source-related particulate matter (PM) in relation to the production of reactive oxygen species (ROS) and cytokine adsorption by particles, Inhal Toxicol, 22 Suppl 2, 37-47, https://doi.org/10.3109/08958378.2010.518377, 2010.

Ayres, J. G., Borm, P., Cassee, F. R., Castranova, V., Donaldson, K., Ghio, A., Harrison, R. M., Hider, R., Kelly, F., Kooter, I. M., Marano, F., Maynard, R. L., Mudway, I., Nel, A., Sioutas, C., Smith, S., Baeza-Squiban, A., Cho, A., Duggan, S., and Froines, J.: Evaluating the toxicity of airborne particulate matter and nanoparticles by measuring oxidative stress potential--a workshop report and consensus statement, Inhal Toxicol, 20, 75-99, https://doi.org/10.1080/08958370701665517, 2008.

Bates, J. T., Fang, T., Verma, V., Zeng, L., Weber, R. J., Tolbert, P. E., Abrams, J. Y., Sarnat, S. E., Klein, M., Mulholland, J. A., and Russell, A. G.: Review of Acellular Assays of Ambient Particulate Matter Oxidative Potential: Methods and Relationships with Composition, Sources, and Health Effects, Environ. Sci. Technol., 53, 4003-4019, https://doi.org/10.1021/acs.est.8b03430, 2019.

Borm, P. J. A., Kelly, F., Künzli, N., Schins, R. P. F., and Donaldson, K.: Oxidant generation by particulate matter: from biologically effective dose to a promising, novel metric, Occup Environ Med, 64, 73-74, https://doi.org/10.1136/oem.2006.029090, 2007.

Calas, A., Uzu, G., Kelly, F. J., Houdier, S., Martins, J. M. F., Thomas, F., Molton, F., Charron, A., Dunster, C., Oliete, A., Jacob, V., Besombes, J. L., Chevrier, F., and Jaffrezo, J. L.: Comparison between five acellular oxidative potential measurement assays performed with detailed chemistry on PM10 samples from the city of Chamonix (France), Atmos. Chem. Phys., 18, 7863-7875, https://doi.org/10.5194/acp-18-7863-2018, 2018.

Charrier, J. G. and Anastasio, C.: Impacts of Antioxidants on Hydroxyl Radical Production from Individual and Mixed Transition Metals in a Surrogate Lung Fluid, Atmospheric Environ. (Oxford, England : 1994), 45, 7555-7562, https://doi.org/10.1016/j.atmosenv.2010.12.021, 2011.

Charrier, J. G. and Anastasio, C.: Rates of Hydroxyl Radical Production from Transition Metals and Quinones in a Surrogate Lung Fluid, Environ. Sci. Technol., 49, 9317-9325, https://doi.org/10.1021/acs.est.5b01606, 2015.

Charrier, J. G., McFall, A. S., Vu, K. K. T., Baroi, J., Olea, C., Hasson, A., and Anastasio, C.: A bias in the "mass-normalized" DTT response – An effect of non-linear concentration-response curves for copper and manganese, Atmospheric Environ., 144, 325-334, https://doi.org/10.1016/j.atmosenv.2016.08.071, 2016.

Chen, X., Zhong, Z., Xu, Z., Chen, L., and Wang, Y.: 2',7'-Dichlorodihydrofluorescein as a fluorescent probe for reactive oxygen species measurement: Forty years of application and controversy, Free Radic Res, 44, 587-604, https://doi.org/10.3109/10715761003709802, 2010.

Cho, A. K., Sioutas, C., Miguel, A. H., Kumagai, Y., Schmitz, D. A., Singh, M., Eiguren-Fernandez, A., and Froines, J. R.: Redox activity of airborne particulate matter at different sites in the Los Angeles Basin, Environ. Res., 99, 40-47, https://doi.org/10.1016/j.envres.2005.01.003, 2005.

Delfino, R. J., Sioutas, C., and Malik, S.: Potential role of ultrafine particles in associations between airborne particle mass and cardiovascular health, Environ. Health Perspect., 113, 934-946, https://doi.org/10.1289/ehp.7938, 2005.

Atmospheric
Measurement
Techniques
Discussions

Open Access

EGU

406 Delfino, R. J., Staimer, N., Tjoa, T., Gillen, D. L., Schauer, J. J., and Shafer, M. M.: Airway inflammation
407 and oxidative potential of air pollutant particles in a pediatric asthma panel, J Expo Sci Environ
408 Epidemiol, 23, 466-473, https://doi.org/10.1038/jes.2013.25, 2013.

409 Dou, J., Lin, P., Kuang, B.-Y., and Yu, J.: Reactive Oxygen Species Production Mediated by Humic-like
410 Substances in Atmospheric Aerosols: Enhancement Effects by Pyridine, Imidazole, and Their
411 Derivatives, Environ. Sci. Technol., 49, https://doi.org/10.1021/es5059378, 2015.

412 Ehhalt, D. H. and Rohrer, F.: Dependence of the OH concentration on solar UV, J. Geophys. Res.:
413 Atmospheres, 105, 3565-3571, https://doi.org/10.1029/1999jd901070, 2000.

414 Eiguren-Fernandez, A., Kreisberg, N., and Hering, S.: An online monitor of the oxidative capacity of
415 aerosols (o-MOCA), Atmos Meas Tech, 10, 633-644, https://doi.org/10.5194/amt-10-633-2017, 2017.

416 Fang, T., Guo, H., Zeng, L., Verma, V., Nenes, A., and Weber, R. J.: Highly Acidic Ambient Particles,
417 Soluble Metals, and Oxidative Potential: A Link between Sulfate and Aerosol Toxicity, Environ. Sci.
418 Technol., 51, 2611-2620, https://doi.org/10.1021/acs.est.6b06151, 2017.

419 Fang, T., Verma, V., Guo, H., King, L., Edgerton, E., and Weber, R.: A semi-automated system for
420 quantifying the oxidative potential of ambient particles in aqueous extracts using the dithiothreitol (DTT)
421 assay: Results from the Southeastern Center for Air Pollution and Epidemiology (SCAPE), Atmos Meas
422 Tech Discussions, 7, 7245-7279, https://doi.org/10.5194/amtd-7-7245-2014, 2014.

423 Fang, T., Verma, V., Bates, J., Abrams, J., Strickland, M., Ebelt, S., Chang, H., Mulholland, J., Tolbert,
424 P., Russell, A., and Weber, R.: Oxidative potential of ambient water-soluble $PM_{2.5}$ in the
425 southeastern United States: contrasts in sources and health associations between ascorbic acid (AA) and
426 dithiothreitol (DTT) assays, Atmospheric Chem. Phys., 16, https://doi.org/10.5194/acp-16-3865-2016,
427 2016.

428 Ghio, A. J., Carraway, M. S., and Madden, M. C.: Composition of air pollution particles and oxidative
429 stress in cells, tissues, and living systems, J. Toxicol. Environ. Health. Part B, Critical reviews, 15, 1-21,
430 https://doi.org/10.1080/10937404.2012.632359, 2012.

431 Guo, Z., Guo, Q., Chen, S., Zhu, B., Zhang, Y., Yu, J., and Guo, Z.: Study on pollution behavior and
432 sulfate formation during the typical haze event in Nanjing with water soluble inorganic ions and sulfur
433 isotopes, Atmos Res, 217, 198-207, https://doi.org/10.1016/j.atmosres.2018.11.009, 2019.

434 Hedayat, F., Stevanovic, S., Miljevic, B., Bottle, S., and Ristovski, Z.: Review – Evaluating the molecular
435 assays for measuring the oxidative potential of particulate matter, Chem Ind Chem Eengq, 21, 31-31,
436 https://doi.org/10.2298/CICEQ140228031H, 2014.

437 Hellack, B., Quass, U., Nickel, C., Wick, G., Schins, R. P. F., and Kuhlbusch, T. A. J.: Oxidative potential
438 of particulate matter at a German motorway, Environ Sci Process Impacts, 17, 868-876,
439 https://doi.org/10.1039/c4em00605d, 2015.

440 Huang, W., Zhang, Y., Zhang, Y., Zeng, L., Dong, H., Huo, P., Fang, D., and Schauer, J. J.: Development
441 of an automated sampling-analysis system for simultaneous measurement of reactive oxygen species
442 (ROS) in gas and particle phases: GAC-ROS, Atmospheric Environ., 134, 18-26,
443 https://doi.org/10.1016/j.atmosenv.2016.03.038, 2016.

444 Janssen, N. A., Strak, M., Yang, A., Hellack, B., Kelly, F. J., Kuhlbusch, T. A., Harrison, R. M.,
445 Brunekreef, B., Cassee, F. R., Steenhof, M., and Hoek, G.: Associations between three specific a-cellular
446 measures of the oxidative potential of particulate matter and markers of acute airway and nasal
447 inflammation in healthy volunteers, Occup Environ Med, 72, 49-56, https://doi.org/10.1136/oemed-
448 2014-102303, 2015.

449 Li, Y., Zhu, T., Zhao, J., and Xu, B.: Interactive enhancements of ascorbic acid and iron in hydroxyl

450   radical generation in quinone redox cycling, Environ. Sci. Technol., 46, 10302-10309,
451   https://doi.org/10.1021/es301834r, 2012.

452   Liu, Q., Baumgartner, J., Zhang, Y., Liu, Y., Sun, Y., and Zhang, M.: Oxidative potential and
453   inflammatory impacts of source apportioned ambient air pollution in Beijing, Environ. Sci. Technol., 48,
454   12920-12929, 10.1021/es5029876, 2014.

455   Liu, X., Zhang, Y. L., Peng, Y., Xu, L., Zhu, C., Cao, F., Zhai, X., Haque, M. M., Yang, C., Chang, Y.,
456   Huang, T., Xu, Z., Bao, M., Zhang, W., Fan, M., and Lee, X.: Chemical and optical properties of
457   carbonaceous aerosols in Nanjing, eastern China: regionally transported biomass burning contribution,
458   Atmos. Chem. Phys., 19, 11213-11233, https://doi.org/10.5194/acp-19-11213-2019, 2019.

459   Lodovici, M. and Bigagli, E.: Oxidative stress and air pollution exposure, J. Toxicol, 2011, 487074,
460   https://doi.org/10.1155/2011/487074, 2011.

461   Pal, A. K., Bello, D., Budhlall, B., Rogers, E., and Milton, D. K.: Screening for Oxidative Stress Elicited
462   by Engineered Nanomaterials: Evaluation of Acellular DCFH Assay, Dose Response, 10, 308-330,
463   https://doi.org/10.2203/dose-response.10-036.Pal, 2012.

464   Perrone, M. G., Zhou, J., Malandrino, M., Sangiorgi, G., Rizzi, C., Ferrero, L., Dommen, J., and
465   Bolzacchini, E.: PM chemical composition and oxidative potential of the soluble fraction of particles at
466   two sites in the urban area of Milan, Northern Italy, Atmospheric Environ., 128, 104-113,
467   https://doi.org/10.1016/j.atmosenv.2015.12.040, 2016.

468   Pöschl, U. and Shiraiwa, M.: Multiphase chemistry at the atmosphere-biosphere interface influencing
469   climate and public health in the anthropocene, Chemical reviews, 115, 4440-4475,
470   https://doi.org/10.1021/cr500487s, 2015.

471   Puthussery, J. V., Zhang, C., and Verma, V.: Development and field testing of an online instrument for
472   measuring the real-time oxidative potential of ambient particulate matter based on dithiothreitol assay,
473   Atmos. Meas. Tech., 11, 5767-5780, https://doi.org/10.5194/amt-11-5767-2018, 2018.

474   Rohrer, F. and Berresheim, H.: Strong correlation between levels of tropospheric hydroxyl radicals and
475   solar ultraviolet radiation, Nature, 442, 184-187, https://doi.org/10.1038/nature04924, 2006.

476   Sameenoi, Y., Koehler, K., Shapiro, J., Boonsong, K., Sun, Y., Collett, J., Jr., Volckens, J., and Henry, C.
477   S.: Microfluidic electrochemical sensor for on-line monitoring of aerosol oxidative activity, J. Am. Chem.
478   Soc., 134, 10562-10568, https://doi.org/10.1021/ja3031104, 2012.

479   Stevanovic, S., Vaughan, A., Hedayat, F., Salimi, F., Rahman, M. M., Zare, A., Brown, R. A., Brown, R.
480   J., Wang, H., Zhang, Z., Wang, X., Bottle, S. E., Yang, I. A., and Ristovski, Z. D.: Oxidative potential of
481   gas phase combustion emissions - An underestimated and potentially harmful component of air pollution
482   from combustion processes, Atmospheric Environ., 158, 227-235,
483   https://doi.org/10.1016/j.atmosenv.2017.03.041, 2017.

484   Stieger, B., Spindler, G., van Pinxteren, D., Grüner, A., Wallasch, M., and Herrmann, H.: Development
485   of an online-coupled MARGA upgrade for the 2 h interval quantification of low-molecular-
486   weight organic acids in the gas and particle phases, Atmos. Meas. Tech., 12, 281-298,
487   https://doi.org/10.5194/amt-12-281-2019, 2019.

488   Velali, E., Papachristou, E., Pantazaki, A., Choli-Papadopoulou, T., Planou, S., Kouras, A., Manoli, E.,
489   Besis, A., Voutsa, D., and Samara, C.: Redox activity and in vitro bioactivity of the water-soluble fraction
490   of urban particulate matter in relation to particle size and chemical composition, Environ. Pollut., 208,
491   774-786, https://doi.org/10.1016/j.envpol.2015.10.058, 2016.

492   Visentin, M., Pagnoni, A., Sarti, E., and Pietrogrande, M. C.: Urban $PM_{2.5}$ oxidative potential: Importance
493   of chemical species and comparison of two spectrophotometric cell-free assays, Environ. Pollut., 219,

Atmospheric
Measurement
Techniques
Discussions

494 72-79, https://doi.org/10.1016/j.envpol.2016.09.047, 2016.

495 Vreeland, H., Weber, R., Bergin, M., Greenwald, R., Golan, R., Russell, A. G., Verma, V., and Sarnat, J.
496 A.: Oxidative potential of PM2.5 during Atlanta rush hour: Measurements of in-vehicle dithiothreitol
497 (DTT) activity, Atmospheric Environ., 165, 169-178, https://doi.org/10.1016/j.atmosenv.2017.06.044,
498 2017.

499 Wang, J., Lin, X., Lu, L., Wu, Y., Zhang, H., Lv, Q., Liu, W., Zhang, Y., and Zhuang, S.: Temporal
500 variation of oxidative potential of water soluble components of ambient $PM_{2.5}$ measured by dithiothreitol
501 (DTT) assay, Sci. Total Environ., 649, 969-978, https://doi.org/10.1016/j.scitotenv.2018.08.375, 2019.

502 Wragg, F. P. H., Fuller, S. J., Freshwater, R., Green, D. C., Kelly, F. J., and Kalberer, M.: An automated
503 online instrument to quantify aerosol-bound reactive oxygen species (ROS) for ambient measurement
504 and health-relevant aerosol studies, Atmos. Meas. Tech., 9, 4891-4900, https://doi.org/10.5194/amt-9-
505 4891-2016, 2016.

506 Xiong, Q., Yu, H., Wang, R., Wei, J., and Verma, V.: Rethinking Dithiothreitol-Based Particulate Matter
507 Oxidative Potential: Measuring Dithiothreitol Consumption versus Reactive Oxygen Species Generation,
508 Environ. Sci. Technol., 51, 6507-6514, https://doi.org/10.1021/acs.est.7b01272, 2017.

509 Yang, A., Jedynska, A., Hellack, B., Kooter, I., Hoek, G., Brunekreef, B., Kuhlbusch, T. A. J., Cassee, F.
510 R., and Janssen, N. A. H.: Measurement of the oxidative potential of $PM_{2.5}$ and its constituents: The effect
511 of extraction solvent and filter type, Atmospheric Environ., 83, 35-42,
512 https://doi.org/10.1016/j.atmosenv.2013.10.049, 2014.

513 Yu, S., Liu, W., Xu, Y., Yi, K., Zhou, M., Tao, S., and Liu, W.: Characteristics and oxidative potential of
514 atmospheric $PM_{2.5}$ in Beijing: Source apportionment and seasonal variation, Sci. Total Environ., 650,
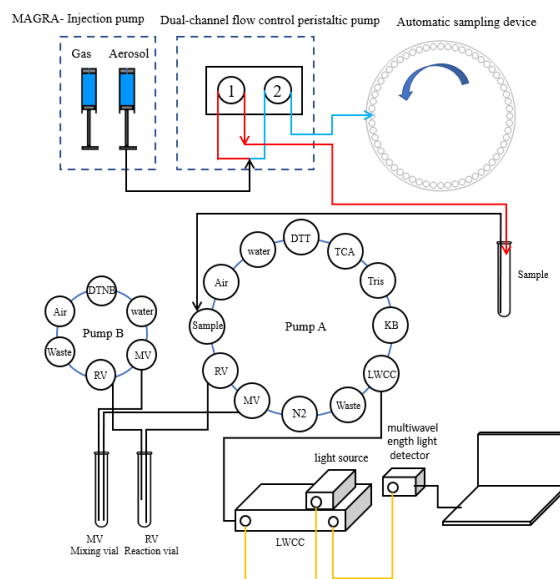515 277-287, https://doi.org/10.1016/j.scitotenv.2018.09.021, 2019.

516 Zhang, C., Yang, C., Liu, X., Cao, F., and Zhang, Y.-l.: Insight into the photochemistry of atmospheric
517 oxalate through hourly measurements in the northern suburbs of Nanjing, China, Sci. Total Environ., 719,
518 137416, https://doi.org/10.1016/j.scitotenv.2020.137416, 2020.

519

520

Atmospheric
Measurement
Techniques
Open Access
Discussions
EGU

521

Figure 1. Automated system setup (Red line: Peristaltic pump 1 runs at a flow rate of 23 ml h^{-1} for the first 4 minutes of each hour; Blue line: Peristaltic pump 2 runs at a flow rate of 27 ml h^{-1} for the remaining 56 minutes of each hour; Yellow line: Optical fiber)
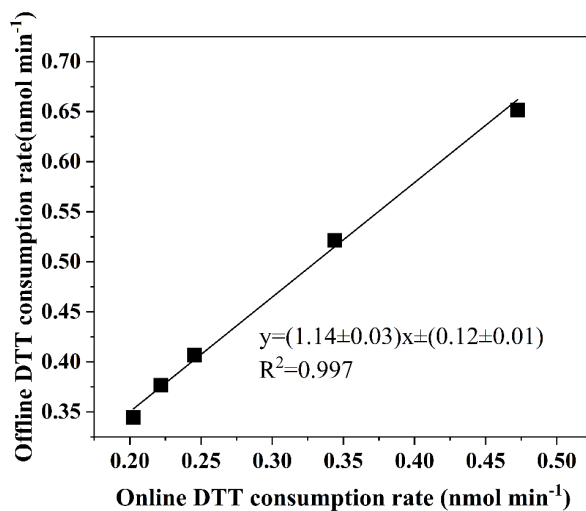

525
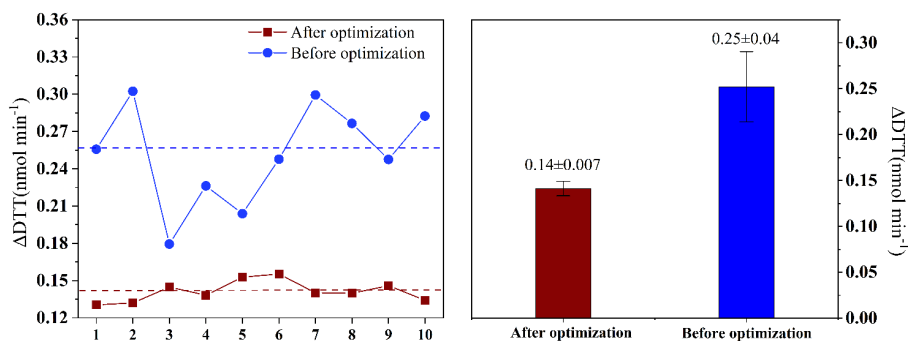
Figure 2. Comparison of blank DTT consumption rate and standard deviation after system optimization (the dotted line is the average value)
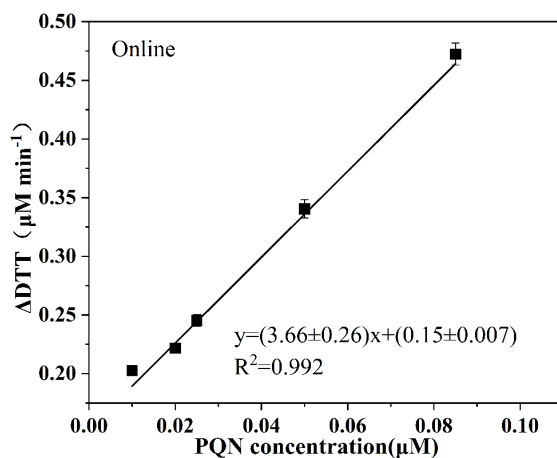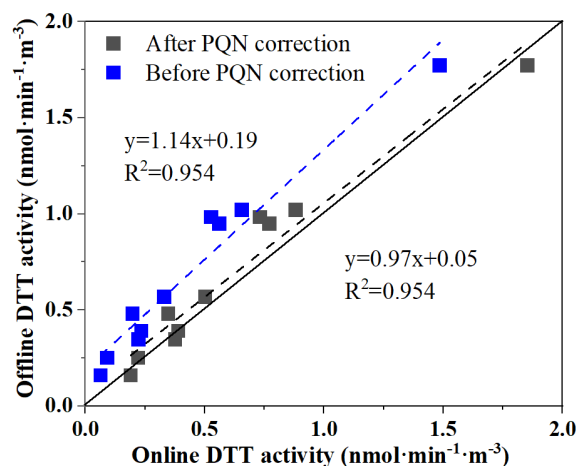
Figure 3.   Blank corrected DTT consumption rate as a function of PQN used as a positive control. Each error bar represents the standard deviation of three independent DTT measurements on each concentration.
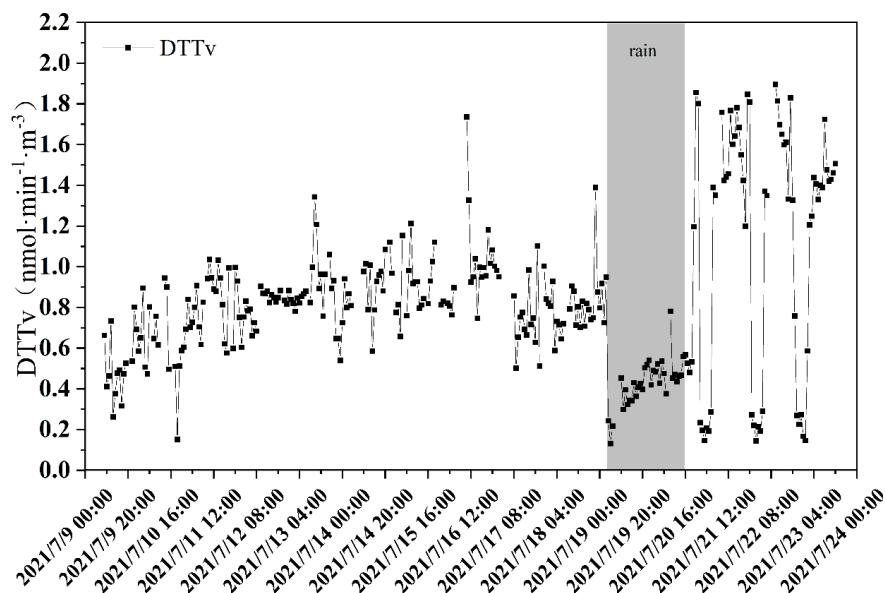

**Figure 4 .** Comparison of the automated system with manual operation using PQN (9,10-phenanthraquinone)

Figure 5. Comparison of the automated system with manual operation using ambient aerosol extracts (PM$_{2.5}$ samples collected from Xuzhou, regression analysis is done by orthogonal regression; the line is 1:1).

Figure 6. Time-series plot of the DTT activity, the shaded part in the figure is the measurement of DTT activity under heavy rain.
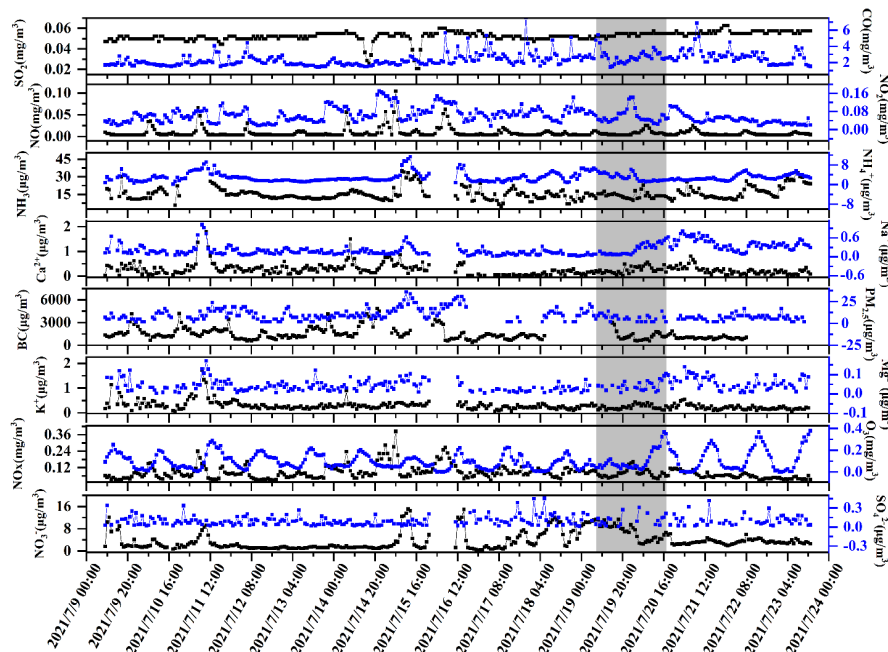
Figure 7. Time series of $PM_{2.5}$ water-soluble components (SO_4^{2-}, NO_3^-, NH_4^+, Na^+, Ca^{2+}, K^+) and polluting gases (SO_2, CO, O_3, NH_3) (The shaded part is rainy weather)

Table 1. The correlation coefficient (R) between the concentration of water-soluble chemical substances in environmental $PM_{2.5}$ ($\mu g\ m^{-3}$) and the volume normalized substance concentration (DTT_V), before rain, during rain, and after rain.

Parameter	Total	Before it rains	During rain	After rain
$PM_{2.5}$	0.014	0.305**	0.026	-0.290*
SO_2	0.195**	0.114	-0.136	0.222
NO	-0.029	-0.029	-0.074	0.050
NO_2	-0.098	0.115	0.169	-0.203
NO_x	-0.085	0.062	0.142	-0.169
CO	-0.033	0.146*	-0.093	0.121
O_3	0.227*	0.153	0.044	0.624**
BC	-0.052	-0.054	-0.439*	0.087
NH_3	0.241**	0.074	-0.129	0.269*
SO_4^{2-}	-0.06	-0.065	0.329	0.028
NO_3^-	-0.163*	-0.155*	-0.352*	0.511**

18

Atmospheric
Measurement
Techniques

Open Access

EGU

Discussions

NH_4^+	0.024	0.028	0.062	0.271*
K^+	-0.077	-0.045	0.125	-0.337**
Mg^{2+}	0.131*	0.075	0.233	0.086
Ca^{2+}	0.005	0.072	0.021	-0.055
Na^+	0.177**	-0.007	0.133	0.008

550     $PM_{2.5}$, particulate matter with an aerodynamic diameter $< 2.5\mu m$; $*P<0.05$, $**P<0.01$.

551